

DIMENSIONAL CHANGE OF 3D PRINTED RESIN WHEN EXPOSED TO
ENVIRONMENTAL LIGHT

A Thesis

By

JONATHAN PARKER HAWLEY

Submitted to the Office of Graduate and Professional Studies of
Texas A&M University
in partial fulfillment of the requirements for the degree of

MASTER OF SCIENCE

Committee Chair,
Co-Chair of Committee,
Committee Members,

Head of Department,

Seok-Hwan Cho
Jenn Hwan Chen
Feng Ming Wang
Emet Schneiderman
Larry L. Bellinger

May 2020

Major Subject: Oral Biology

Copyright 2020 Jonathan P. Hawley

ABSTRACT

Statement of problem. To our knowledge, the linear dimensional stability of the SLA 3D printed resins when exposed to environmental light after printing has not been studied. Ideally, the cured resins should have a similar dimensional stability of historically used dental lab materials like type III, IV, and V dental stones.

Purpose. The purpose of this study was to investigate the dimensional changes of 3D printed resin models when exposed to ambient light after post processing.

Materials and Methods. A partially edentulous typodont was scanned to include teeth #18-22. Twenty resin models were printed with a 3D printer. Ten models were stored in ambient light, while ten models were stored in a dark box. Measurements were taken at 0, 12, 24, 48, 96, and 168 hours with a desktop scanner. Measurements were compared using best fit analysis in CAD software. Statistics included mean of models changes over time (student t), mean deviations of model per location (Mann-Whitney U), and Pearson correlation of the initial and final scans.

Results. The average of the means: Group L (light) was $92.18/-108.62 \pm 150.40 \mu\text{m}$; Group D (dark) was $110.12/-73.41 \pm 128.53 \mu\text{m}$. Neither group means were clinically significant ($P > .05$). The means \pm standard deviations of dimensional change for Cusp locations were $147.11 \pm 36.96 \mu\text{m}$ for Group L and $143.32 \pm 11.73 \mu\text{m}$ for Group D; for fossa location were $139.94 \pm 35.98 \mu\text{m}$ for Group L and $134.63 \pm 11.30 \mu\text{m}$ for Group D; for Axial location were $78.56 \pm 21.70 \mu\text{m}$ for Group L and $72.04 \pm 8.10 \mu\text{m}$ for Group D. However, there were not statistically significant differences between groups or among locations ($P > .05$). There was a strong positive correlation between the initial scan and final scan of each models ($P < .001$).

Conclusions. Within the limitations of this study, the recommended printing and post-cure processing provides a linear stable model unaffected by environmental ambient light.

ACKNOWLEDGEMENTS

I would like to thank my directors, Dr. Seok-Hwan Cho and Dr. William Nagy, for their guidance through the program. I would also like to thank the faculty and staff of the Graduate Prosthodontic Clinic at Texas A&M University College of Dentistry. Third, my co-residents who have encouraged, taught, and directed me to be a better prosthodontist. Lastly, I'd like to thank my wife and family for their support of seven years in dental school and residency.

CONTRIBUTORS AND FUNDING SOURCES

Contributors

The work of this thesis was overseen and supported the thesis committee: Dr. Seok-Hwan Cho (committee chair), Dr. Jenn-Hwan Chen, Dr. Feng Ming Wang, and Dr. Emet Schneiderman.

Data analysis was in part provided by Dr. Emet Schneiderman.

All other work conducted for the thesis was completed by the student independently.

Funding Sources

Texas A&M University Department of Graduate Studies provided the funding necessary to complete the original research.

NOMENCLATURE

AM	Additive manufacturing
SM	Subtractive manufacturing
STL	Standard Tessellation Language
SLA	Stereolithography
DLP	Digital Light Processing
IPA	Isopropyl Alcohol
CAD/CAM	Computer Aided Design/Computer Aided Manufacturing

TABLE OF CONTENTS

	Page
ABSTRACT	ii
ACKNOWLEDGEMENTS	iii
CONTRIBUTORS AND FUNDING SOURCES	iv
NOMENCLATURE.....	v
TABLE OF CONTENTS	vi
LIST OF FIGURES	vii
INTRODUCTION	1
MATERIALS AND METHODS.....	5
RESULTS.....	10
DISCUSSION.....	17
CONCLUSIONS	22
REFERENCES	23

LIST OF FIGURES

	Page
Figure 1. STL of scanned typodont (left) and trimmed typodont (right).....	5
Figure 2. The study design.	6
Figure 3. Statistical analysis example for all groups.	7
Figure 4. Example of best fit analysis and alignment in Geomagic.	8
Figure 5. 39-point selection on one of the twenty models.	8
Figure 6. Mesh point view of STLs.	11
Figure 7. Relative values (μm) of positive (expansion) & negative (shrinkage) changes.	12
Figure 8. Deviation at locations by time.	14
Figure 9. Pearson correlation for each model axis.....	16
Figure 10. Micron comparison.	19

INTRODUCTION

It is well known in dentistry the quality of the dental restoration is based on the control of compounding factors such as accurate impression making, fabrication of custom trays 24 hours prior to impressions, and being cognizant of the delayed linear expansion of dental stone¹⁻³. A fast-paced advancement of 3D desktop printers has opened up new and exciting opportunities for dentistry.^{4,5} One example is printing resin models in-office based on intra-oral and/or bench top scanners in comparison with taking conventional impressions and pouring in dental stone.^{6,7}

Ideal properties of impression materials are accuracy, elastic recovery, dimensional stability, flow, flexibility, workability, hydrophilicity, long shelf-life, patient comfort, and economics.¹ ADA specification #19 requires elastomeric materials to reproduce fine details of 25 μm and gypsum die material is required to reproduce details at 50 μm . Contrasting conventional impression and model materials, intraoral scanners and printed models may negate some of these ideal properties. Intraoral scanners have been reported to reproduce details as small as 7 μm on partial arch and 21 μm on whole arch scans.⁶ There is no need for elastic recovery or rebound with intraoral scanner since it is a touchless scan eliminating distortion like physical impressions. Additionally, intraoral scans are virtually stable in the file format and 3D printed models may supersede die stone for some dental procedures. 3D printed resin models do not need properties such as flow, flexibility, workability, hydrophilicity, and/or shelf-life as conventional dental stone. Lastly, it has also been reported patient comfort, satisfaction, and preference is high with intraoral scanners compared to conventional alginate impressions.⁸

Computer-aided design/computer-aided manufacture (CAD/CAM) was first introduced to dentistry in 1970's by Duret and Preston.^{6, 10} After its introduction it began to enter more dental labs and offices in the 1990's and early 2000's until it has become commonplace.¹¹ All CAD/CAM technology have three phases: data acquisition, computer-aided design (CAD), and computer-assisted manufacture (CAM). Once an object reaches CAM it can either be manufactured by subtractive (SM) or additive (AM) processes. SM, or milling, starts with a larger block or puck and utilizes a series of burs to remove material to the required dimensions. Examples of SM in the dental field are Avadent dentures and Ivoclar IPS emax ZirCAD Prime. AM, or 3D printing, uses material deposition in a layer by layer process to create objects with much less material when compared to SM.¹² Examples of AM are 3D printers like FormLabs Form2 SLA and SprintRay MoonRay DLP, and 3D-RPD laser sintering of chromium-cobalt for partial dentures.

Currently, there are three main types of AM CAM, or 3D printing techniques, utilized in dentistry: direct deposition, laser sintering, and photopolymerization.⁴ Direct deposition can use powder (binder jetting), slurry (material jetting), or photopolymerized resin (DLP-jetting). Most direct deposition printing in dentistry is used for dental models. Laser sintering is most commonly used for metal, such as removable partial dentures fabricated by 3D-RPD. Photopolymerization includes the most commonly used dental in-office 3D printers: stereolithography (SLA) and digital light processing (DLP). Both printers use an ultra-violet light to activate photoinitiators in the resins, which bond or harden the liquid into a solid state of sequential layers.⁵ The main difference between these two types of 3D printers is SLA cures resin with a single laser point forming layers over several seconds to minutes versus DLP cures

with a laser in entire planes using a digital micromirror device curing resin at a quicker rate.^{4, 5, 9} SLA and DLP printers can be used to print surgical guides, resin patterns, temporary restorations, dental models, castings, wax patterns, etc. Advantages of SLA are high accuracy, smooth surface finish, possible transparent objects, good mechanical strength, fine build details, low tolerance. Disadvantages of SLA are expensive, high material cost, only photopolymerized material available, post curing required, and single material vats. Advantages of DLP are fast printing, smooth surface finish, possible transparent objects, and fine build details. Disadvantages of DLP are only photopolymerized material, post curing required, and single material vats.^{4, 5}

Three important aspects of 3D printing are accuracy, precision, and trueness.¹³ Accuracy incorporates both precision and trueness (ISO 5725-1).¹⁴ Precision describes the proximity of each measurement, i.e. how close are each of the measurements. Trueness describes the distance of the measurement from the actual object, i.e. how far away from the real measurement.¹⁵ A precise measurement correlates with repeatability. A true measurement correlates with duplication of the measured object. It has been shown the scanner used in this study, 3Shape D900, is accurate in regards to precision and trueness.^{6, 22}

According to the manufacturer, FormLabs, the dental model resin is accurate within $\pm 35 \mu\text{m}$ over eighty percent of the surface points if printed at $25 \mu\text{m}$ printer settings.¹⁶ Goodacre et al. have shown 3D printing is accurate and precise for dental uses.¹⁷ Similar studies by other authors have confirmed also.¹⁸⁻²¹

For model resin, FormLabs recommends: 1) design thickness, 2) print orientation, and 3) post processing. For design thickness wall thickness of 2.0 mm minimum value to ensure structural stability.²² For print orientation, the model should be oriented with the intaglio surface of the model facing the build platform to allow supports to be attached to non-critical areas. Post processing includes washing the models with 99% isopropyl alcohol (IPA), preferably in the Form Wash for 20 minutes, followed by air drying for 30 minutes or compressed air until visually dry.²³ Lastly, inserting the models into Form Cure for 60 minutes at 60°C to increase the tensile modulus by as much as 72%.²⁴ Once post-processing is complete, then remove the supports and lightly polish areas if needed.²²

The American Dental Association (ADA) states in specification 25 that improved dental stone final setting expansion is made two hours after mixing, but has been shown to continue changing up to 120 hours.³ This has been defined and reported as the linear dimensional stability of dental materials. To our knowledge, the linear dimensional stability of the SLA 3D printed resins when exposed to additional environmental light after printing has not been studied. Ideally, the cured resins should have a similar dimensional stability of historically used dental lab materials like type III, IV, and V dental stones.¹ The purpose of this research project is to investigate the dimensional changes of 3D printed resin models when exposed to ambient light after post processing.

MATERIALS AND METHODS

A typodont with a single missing tooth #19 was used for original scan obtain (M-PVR-1560EC; Columbia Dentoform Corp.). This model was scanned with CAD spray (Renfert-Scanspray; Renfert) in a lab scanner (D900 scanner; 3Shape). The D900 contains four 5.0-megapixel cameras for a non-touch scan to produce a standard tessellation language or stereolithography (STL) file. This allows the virtual recreation of the surface geometry of three-dimensional objects through point clouds, or three axis relation (X, Y, and Z axis).

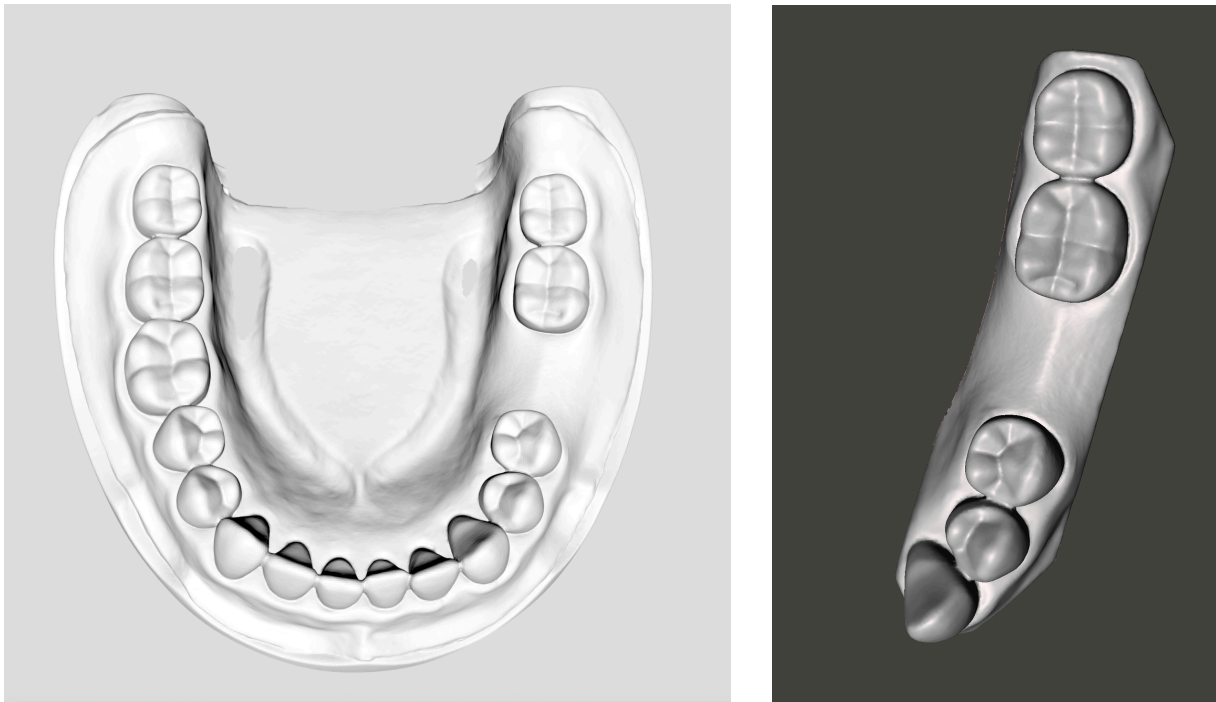


Figure 1. STL of scanned typodont (left) and trimmed typodont (right).

The typodont STL was trimmed in Meshmixer (Autodesk Research) to include lower left quadrant teeth #18-22 with edentulous area at site #19. Both the untrimmed and trimmed

typodont can be seen above in Figure 1. This file was the master cast to print twenty models, ten for each group. Group L will be referred to as “light” and placed on the desktop with exposure to environmental, ambient light after post processing. Group D will be referred to as “dark” and stored in a dark box with no exposure to additional light after post processing. Figure 2 outlines the overall study design. Group L was stored in ambient light and group D was stored in a blackout storage container. All twenty models were printed with Preform software (FormLabs) on Form2 SLA (FormLabs) and dental model resin. Models were printed hollow with 2 mm walls and no base to simulate a similar clinical scenario. The models were then scanned initially (0 hours), 12, 24, 48, 96, and 168 hours. Specimens will be scanned with the 3Shape D900 desktop scanner at varied time intervals similar to the study completed in 2002 by Heshmati et al.³ The initial scan (0 hours) was used as the master comparison model as seen in Figure 3.

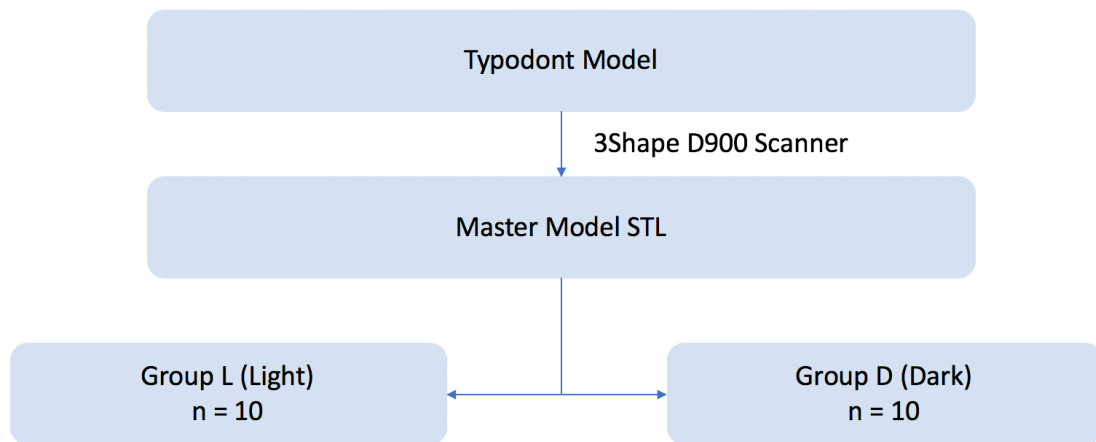


Figure 2. The study design. Typodont model scanned and virtually trimmed to make master STL for printer accuracy comparison and all twenty model prints. The models were then split into groups of ten for Group L (Light) and Group D (Dark).

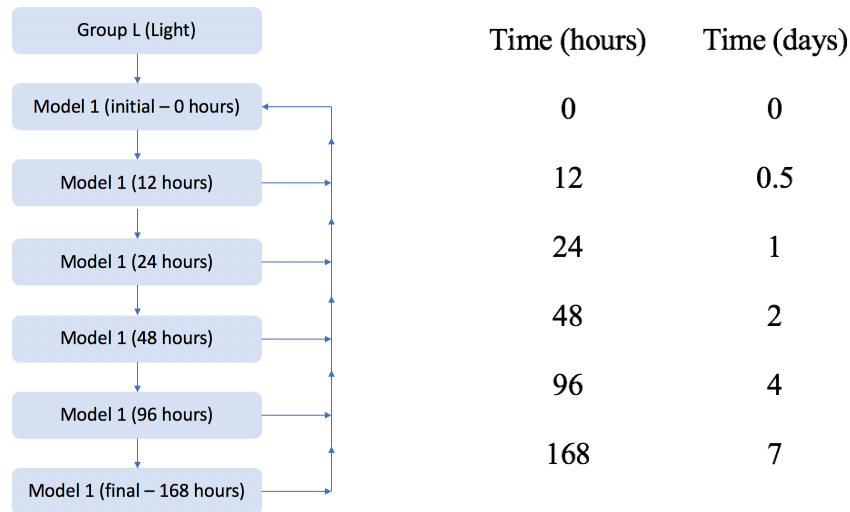


Figure 3. Statistical analysis example for all groups. Group L shown here. Models at each time interval were compared to the initial (0 hour) scan to determine dimensional changes. Measurements were made with 3Shape D900 desktop scanner at time 0, 12, 24, 48, 96, and 168 hours.

Specimens were compared by using surface analysis software (Geomagic Control 2014; 3D systems) to analyze dimensional changes with a best fit algorithm.^{25, 26} The best fit algorithm is a virtual alignment based on the STL point cloud surface matching to maximize the amount of matching surface data points while minimizing the amount of deviations. This is set automatically in the program but can be manually changed. The input was as follows: 1 mm specimen points for sample size 5,000 points with a 100 μm maximum deviation, 35 μm critical value, and 50 μm maximum nominal value. The example of a reference and test models best fit alignment can be seen below in Figure 4. A similar protocol for discrepancies followed Goodacre et al. who used 64-points of measurement with 1mm diameter on an entire arch.¹⁷ The present study was a quadrant and thus decided to used approximately half as many locations as

Goodacre for a total of 39-points of measurement. An example of one of the models with all 39 points is below in Figure 5.

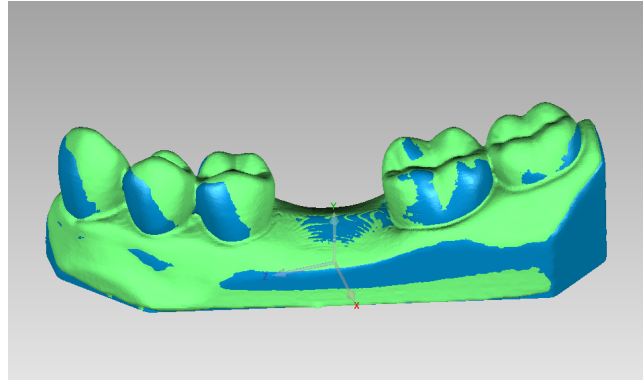


Figure 4. Example of best fit analysis and alignment in Geomagic. Blue model is the initial scanned model (reference) at time zero hours. Green model is the new model (comparison) after best fit analysis. The ideal alignment is a “cameo” style blue as seen at the crest of the ridge of #19 edentulous area.

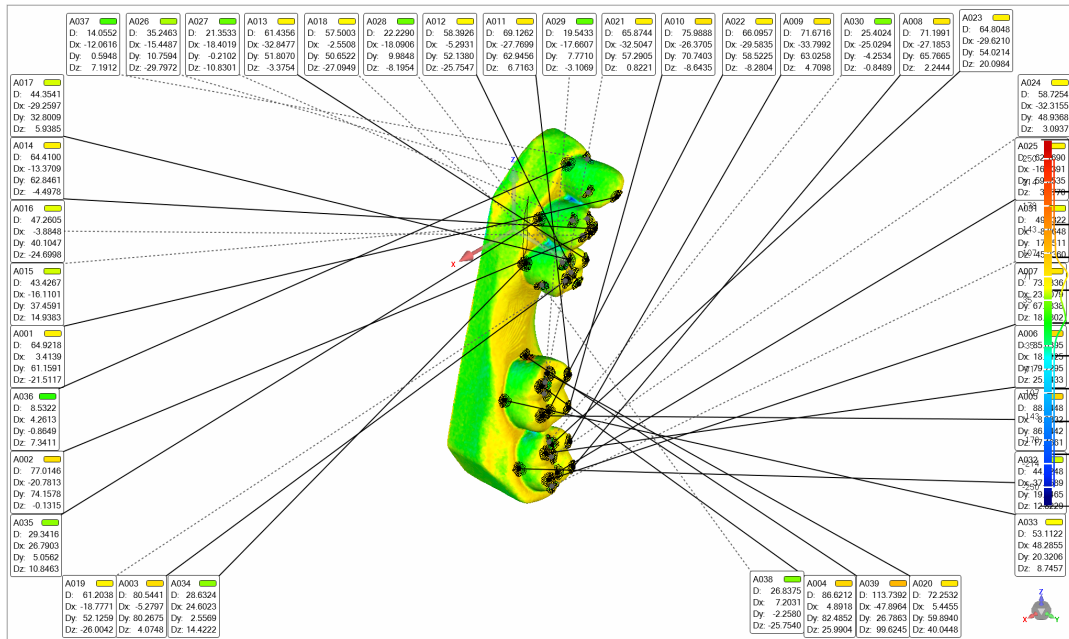


Figure 5. 39-point selection on one of the twenty models. Locations were divided into cusp tips (14 measurements), fossa (10 measurements), and axial walls (15 measurements).

Geomagic output was recorded in Microsoft Excel and subsequent statistical testing was completed with SPSS, IBM. Four statistical tests were completed: 1) student t test for the printer error of the models at time zero to original STL, 2) student t test for mean of printed models compared to the printed model at time zero hours, 3) Mann-Whitney U for absolute mean of deviations per location of cusps, fossae, and axial walls, per time group and 4) Pearson Correlation between models at initial scan to final scan in the X-, Y-, and Z-axis.

RESULTS

A qualitative analysis was completed by using heat maps, wire frame renderings, and point clouds produced with Geomagic software. The following statistical tests were run for quantitative analysis: student t-test, Mann-Whitney U, and Pearson Correlation.

The color map for the qualitative analysis can be seen below in Figure 6. Noted is the unproportionate concentration of point cloud data at the edentulous site #19, i.e. the black area compared to the green wire mesh of the surrounding model. The critical value was set at 35 μm , which is the manufacturer published accuracy. Red color mapping are positive discrepancies showing areas of the model which are above or in front of the test comparison. Blue color mapping are negative discrepancies showing areas of the model which are behind or below the test comparison. Green, yellow-green, and aqua colors are relatively normal, i.e. acceptable error. Most of the model surface is green, yellow-green, and/or aqua colors. The largest color map error appears farther distal from the designated missing #19 area, e.g. #17 occlusal surface and #22 cusp tip. As seen in the spectrum graph in Figure 10 (right) a majority of deviations are relatively gathered around +35 and -35 μm with a normal bell-shaped curve distribution. There appears to be a slight tendency towards positive error in the best fit alignment as evident from the peak of the bell-shape curve at approximately +50 μm .

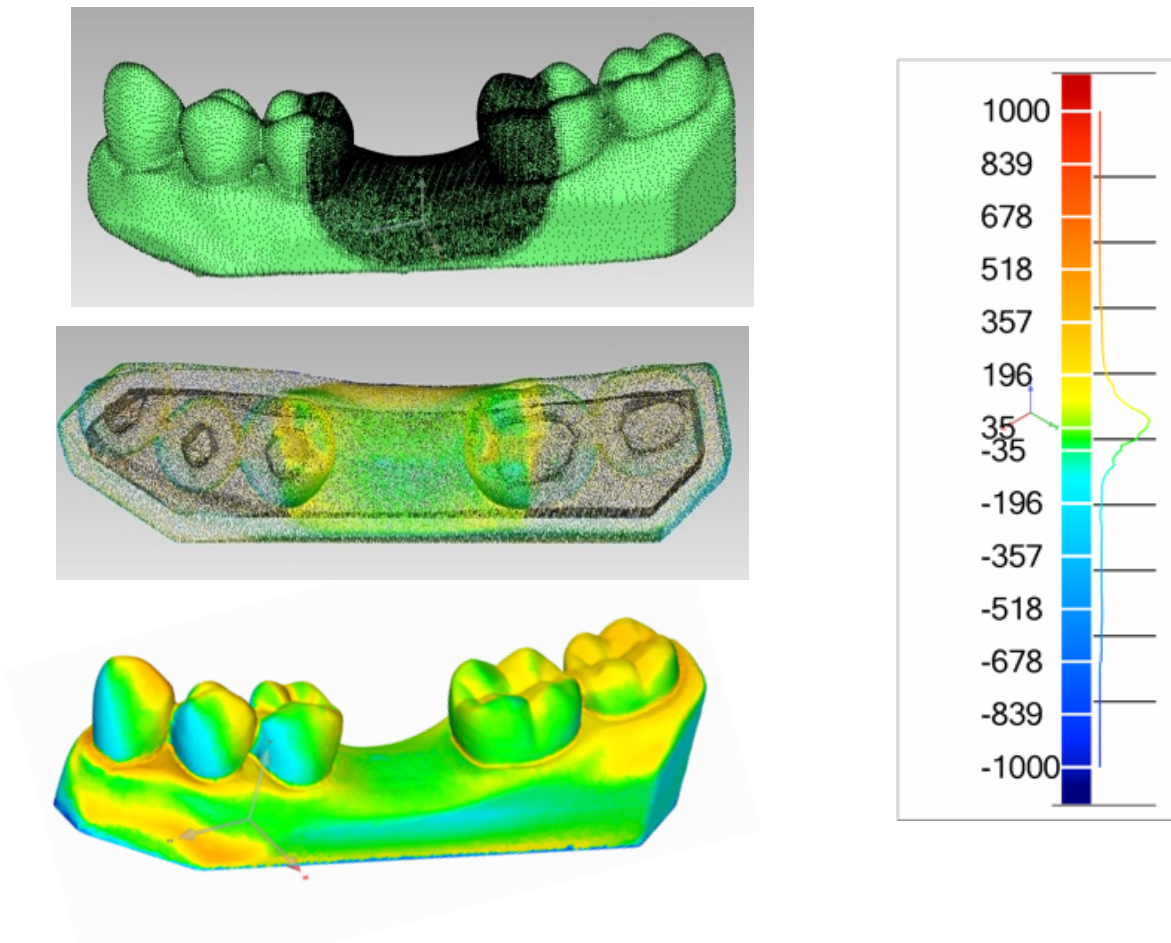


Figure 6. Mesh point view of STLs. Emphasizing the concentration at #19 edentulous area (top) with best fit analysis (middle) and heat map of deviations (bottom and right).

The printer error was calculated by comparing the printed resin model at time zero hours to the original STL file. For Group L the printer error was $123.5 \pm 185 \mu\text{m}$ and Group D was $115.1 \pm 207 \mu\text{m}$. The student t-test for the printer error showed it to not be statistically significant between groups ($P > .05$)

The second student t-test was used to determine the difference in models over time compared to the original scanned model at time zero hours (i.e. 12-0, 24-0, 48-0, etc.). This value showed

positive (expansion) and negative (shrinkage) in microns. Results for both Group L and Group D are shown in Figure 7. The means for Group L (light) for time 12, 24, 48, 96, and 168 hours were 103.6/-104.8, 54.3/-45.6, 82.7/-86.5, 59.9/-133.7, and 161.0/-172.5 \pm 150.40 μ m, respectively. The mean for Group D (dark) for time 12, 24, 48, 96, and 168 hours were 132.6/-57.2, 133.9/-114.1, 86.4/-69.6, 107.9/-60.3, and 89.8/-65.9 \pm 128.53 μ m, respectively. The results for either group were not clinically significant ($P > .05$).

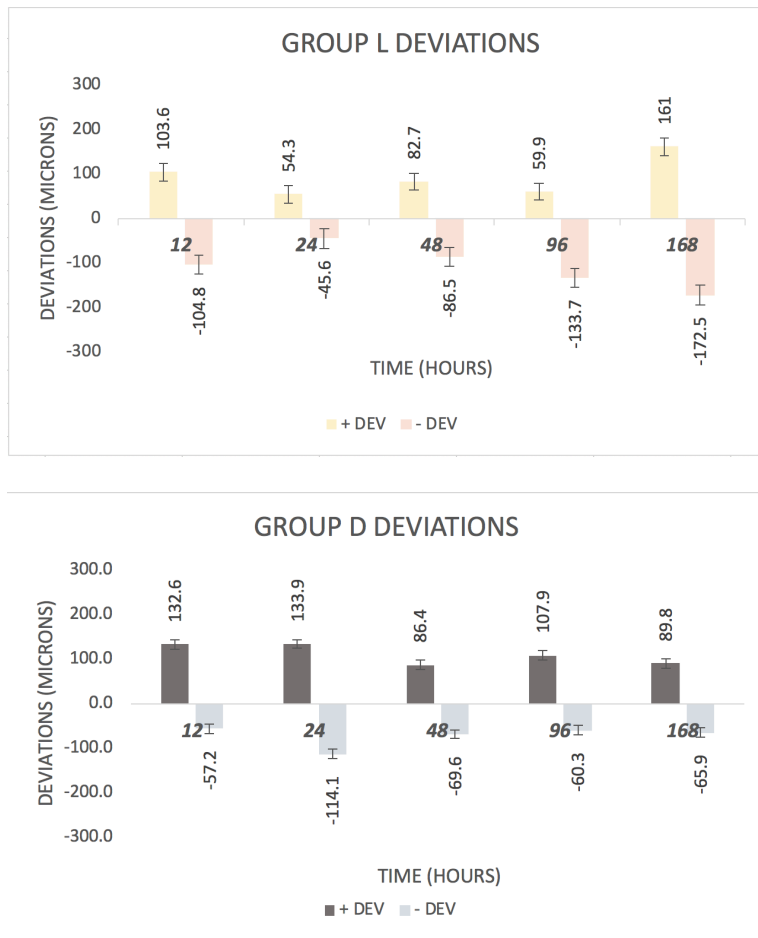


Figure 7. Relative values (μ m) of positive (expansion) & negative (shrinkage) changes.

A 39-point comparison and Mann-Whitney U statistical test was used to evaluate the changes of specific areas such as cusp tips (14 measurements), fossa (10 measurements), and axial walls (15 measurements). Results were analyzed comparing the time groups, 12, 24, 48, 96, and 168 hours, and can be seen below in Figure 8. The mean for 12, 24, 48, 96, 168 hours for the Group L at the Cusp location was 175.39, 75.06, 139.34, 73.04, and $272.75 \pm 36.96 \mu\text{m}$, respectively. For Group D at the Cusp location was 151.73, 175.51, 107.48, 154.16, and $127.72 \pm 11.73 \mu\text{m}$, respectively. The total mean for Group L at Cusp location was $147.11 \pm 36.96 \mu\text{m}$ and Group D was $143.32 \pm 11.73 \mu\text{m}$. The mean for 12, 24, 48, 96, 168 hours for the Group L at the Fossa location was 171.91, 69.6, 127.81, 69.01, and $261.38 \pm 35.98 \mu\text{m}$, respectively. For Group D at the Fossa location was 140.75, 166.27, 100.15, 145.67, and $120.30 \pm 11.30 \mu\text{m}$, respectively. The total mean for Group L at Fossa location was $139.94 \pm 35.98 \mu\text{m}$ and Group D was $134.63 \pm 11.30 \mu\text{m}$. The mean for 12, 24, 48, 96, 168 hours for the Group L at the Axial location was 87.38, 42.72, 64.73, 39.69, and $158.29 \pm 21.70 \mu\text{m}$, respectively. For Group D at the Axial location was 80.48, 83.72, 46.56, 89.56, and $59.88 \pm 8.10 \mu\text{m}$, respectively. The total mean for Group L at Axial location was $78.56 \pm 21.70 \mu\text{m}$ and Group D was $72.04 \pm 8.10 \mu\text{m}$. In general, both Groups L and D appear to show deviations at all time periods with neither showing greater or more changes than the other. Also, in general, the axial locations showed the least amount of changes compared to the cusp and fossa locations. None of the deviations between groups or among locations were statistically significant ($P > .05$).

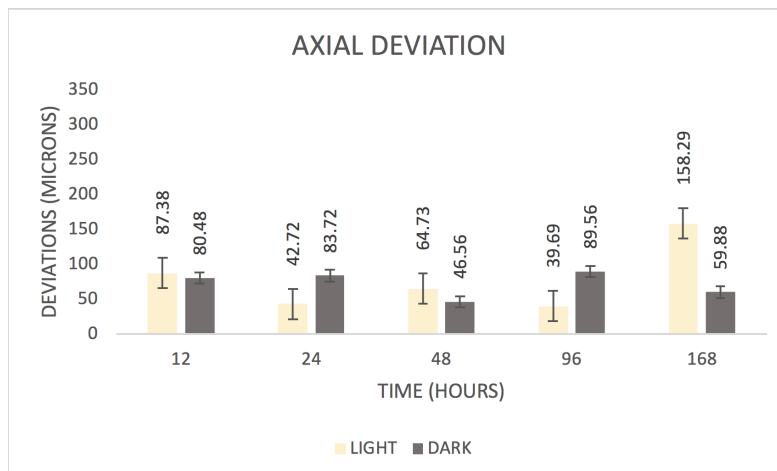
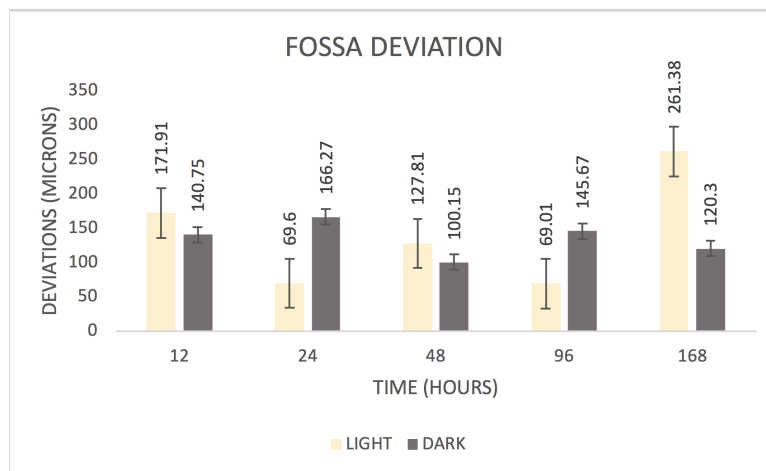
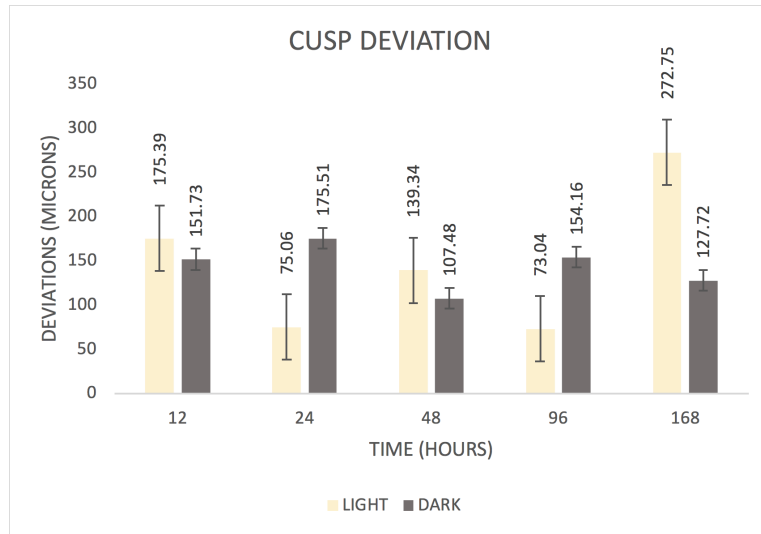
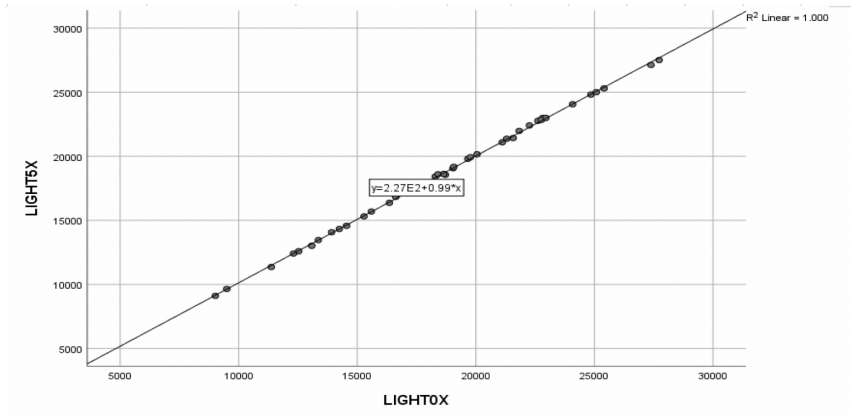


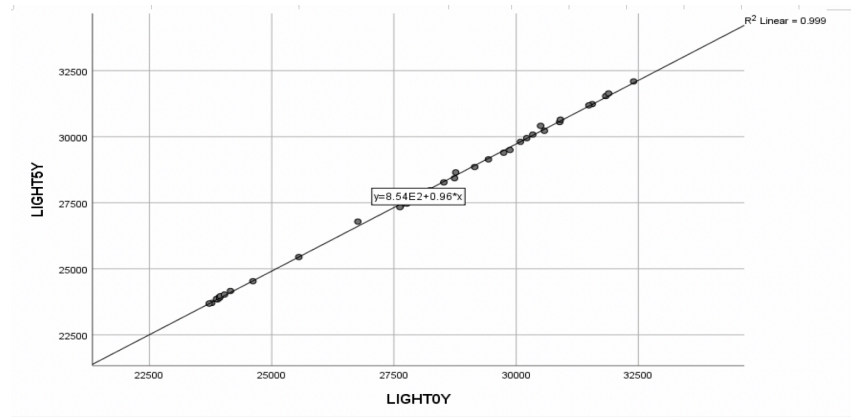
Figure 8. Deviation at locations by time. Cusp (top), fossa (middle), and axial (bottom). No consistent patterns appear between Groups L and D deviations. Axial deviations showed the least deviation compared to cups and fossa measurements. There were no significant differences between groups or among locations.

The last comparison was the Pearson Correlation to show the correlation between measurements at time 0 (0 hours) to time 5 (168 hours). Results are shown in Figure 9. Model measurements for both groups in the X-, Y-, and Z-axis at time 0 (immediate scan) and time 5 (168 hours, 1 week) have a strong positive statistically significant linear relationship ($P < .001$) That is, the models within each group showed no significant dimensional changes from initial scan (0 hours) to final scan (168 hours).

CORRELATION OF X-AXIS



CORRELATION OF Y-AXIS



CORRELATION OF Z-AXIS

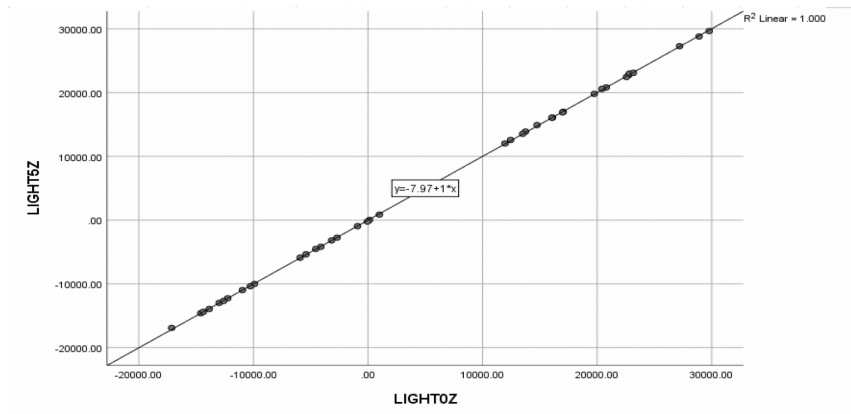


Figure 9. Pearson correlation for each model axis. X (top), Y (middle), and Z (bottom). This confirms the models did not change over time and were statistically significant equal at the initial and final scans.

DISCUSSION

This in vitro study investigated the linear dimensional stability of the SLA 3D printed resins when exposed to additional environmental UV light after printing. The evaluation of accuracy and reproducibility of printed resins revealed there were not significant differences to the resin models when exposed to ambient light. Therefore, the null hypothesis was rejected and the alternative hypothesis was failed to be rejected. The analysis of model movement based on location showed relatively small, equal movement but not in a clinically significant amount.

The American Dental Association (ADA) states in Specification 25 the final setting expansion of dental stone is made two hours after being mixed. Heshmati *et al* reported the amount of linear expansion varied by dental stone manufacturer with some showing the greatest amount after the first two hours.³ They showed all stones completed expansion, the critical time, at 96 hours. This study of 3D printed resins differed with no significant linear expansion or shrinkage within 168 hours. That is, the printing and manufacturer recommended post-processing creates a dimensional stable product even when exposed to additional ambient UV light.

Shwartz *et al* reported on the linear dimensional accuracy of epoxy resin as a stone die substitute with higher resistance to fracture and abrasion.²⁷ They concluded that epoxy resin is comparable to stone dies but may exhibit smaller values in a height (incisogingival dimension) and greater values in a width (buccal-lingual dimension). The 3D printed model resin used in this study potentially could be used to overcome the disadvantages of dental stone and epoxy resin.

Jang et al evaluated the marginal and internal fit of crowns fabricated on a 3D printed model in 2018.⁸ They compared the 3D printed model dies with a conventional dental stone and virtual die. The reported mean value for marginal discrepancy was 30.9 μm and internal gap of 52.6 μm . Most importantly, the fit of the crowns on the 3D printed models (3Dent dental model printer, EnvisionTEC, Gladbeck, Germany & Polyjet Objet EDEN260V, Stratasys LTD Eden Prairie, MN, USA) were inferior to those on the conventional stone model and virtual dies. Therefore, as accurate as the models appear to be in previous and this current study, it is necessary to increase the accuracy of printing models and dies before we are able to fabricate dental restorations directly on the models. However, other options such as milling directly from the CAD file (i.e. STL, OBJ, PLY) avoids the need for a printed model.

Microns are a common measurement in dental research but can be an abstract comparison concept. Figure 10 shows the size comparison in microns of various objects. The average human hair is estimated to be between 80-100 μm . The human eye is able to see particles larger than 50-60 μm . The average size of a single *streptococcus mutans* is 0.5 - 0.75 μm . With these comparative measurements in mind, the relative critical value for marginal gap of dental restorations is 120 μm with a good marginal fit ranging between 40-100 μm .⁸ The printer manufacturer of this study, FormLabs, claims the dental model resin is accurate within ± 35 μm over eighty percent of the surface points if printed at 25 μm printer settings.¹⁶

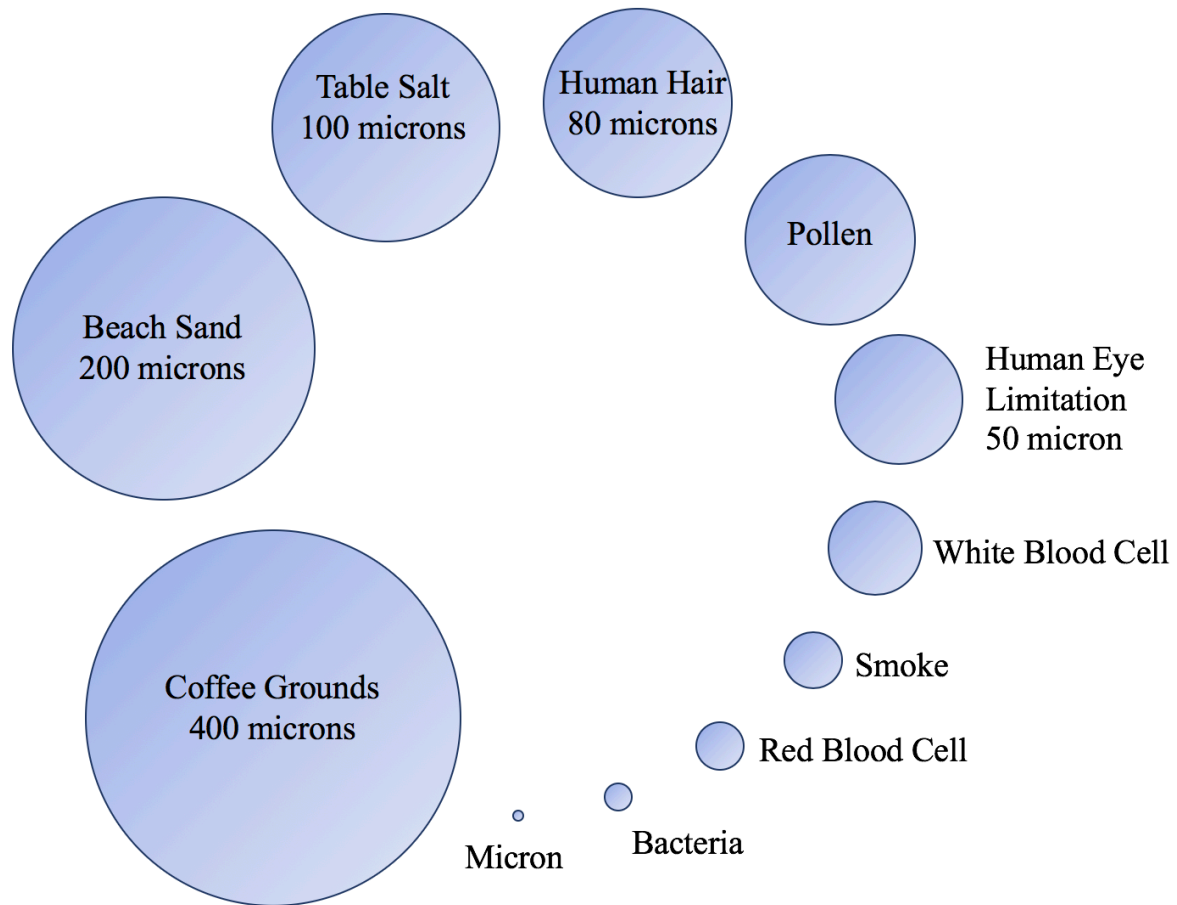


Figure 10. Micron comparison. Human eye limitation is 50 μm . Clinically acceptable restoration margin gap is 120 μm .⁸

The three location comparisons revealed relatively equal changes between both Group L and D at all measurement times. Minor deviations between measurement times are seen in both groups with no distinct trend in either. Possible explanation for the fluctuant measurements of both groups could be either the scanner accuracy and/or the software best-fit algorithm. No pattern in the location comparison in addition to the near perfect strong positive correlation of the Pearson Correlation supports the theory environmental light had no effect on the model expansion or shrinkage over time. Therefore, the 3D printed resin models can be considered stable.

Currently, there are several companies offering in-office 3D printing options: FormLabs (Form2, Form3), SprinRay (MoonRay S), Asiga (Pro, Max), Straumann (Cares P series), etc.

Additionally, there are larger laboratory printers like the Stratasys (Objet30, Eden260VS, Objet260, J720, J700, Objet500), EnvisionTEC (PCA 2000, ONE CDLM, P4K, Vida UHD, PPS DLP, Extreme HD 3SP, etc.), Carbon (Carbon3D), etc. These printers offer options such as dental and orthodontic models, castable fixed partial dentures, direct fixed partial dentures, night guards, surgical guides, denture bases, denture teeth, and many other options. The resins come in various colors, strengths, opacities, and applications. At the time of this research Carbon, which can be used as both in-office and laboratory printer, released in conjunction with Dentsply Sirona a printable Lucitone 199 resin and will print a denture base in 13 minutes. This print time is significantly less than the current in-office standard and strength comparison substantially greater.

The limitations of study are the relatively small sample size of ten models per group and the use of a single printer with only one resin. Initially multiple printers and resins were intended to be analyzed but removed due to access, financial limitations, and scanner limitations of the transparent surgical guide resin. Furthermore, it was noticed the 3Shape software with the D900 had a greater concentration of point clouds (STL values) with the selected edentulous area (i.e. #19). This area had a larger number of comparison points, which possibly resulted in a greater aggregation of the best-fit analysis. This can be seen visually on the point and heat maps in Figure 11. The largest deviations were observed on the distal portions of the models (i.e. #18 and #22), both areas with fewer point clouds compared to the selected edentulous sites (#19).

Lastly, the Geomagic software used to analyze the models was an outdated version no longer supported by the manufacturer. The information technology department of the school denied the request to install the program update due to possible risk of patient health information. Further studies of linear dimensional stability of other printers, resins, and protocols is recommended.

CONCLUSIONS

Within the limitations of this in vitro study the following conclusions may be drawn:

1. There were no statistically significant differences ($P > .05$) of the dimensional change of between Group L and D, up to 168 hours. Group L averaged $92.3/-108.6 \pm 150.40 \mu\text{m}$. Group D averaged $110.12/-73.4 \pm 128.53 \mu\text{m}$.
2. There were no statistically significant differences ($P > .05$) of dimensional change of the 3D printed models at varying locations (cusp tips, fossa, axial walls) between the two groups.
3. There was a strong correlation between models at the initial time (0 hours) and final scan (168 hours) of the 3D printed models. That is, the resin was stable and the models did not change due to subsequent exposure to environmental light ($P > .001$).

REFERENCES

1. Donovan, T. A review of contemporary impression materials and techniques. *Dent Clin N Am* 2004;48:445-70.
2. Goldfogel, M. Dimensional change of acrylic resin tray materials. *J Prosthet Dent* 1985;54:284-86.
3. Heshmati, R. Delayed linear expansion of improved dental stone. *J Prosthet Dent* 2002;88:1.
4. Alharbi, N. Additive manufacturing techniques in prosthodontics: Where do we currently stand? A clinical review. *Int J Prostho* 2017;30;5.
5. Revilla-Leon, M. Additive manufacturing technologies used for processing polymers: current status and potential application in prosthetic dentistry. *J of Prostho* 2019;28:146-58.
6. Abduo, J. Accuracy of intraoral scanners: a systematic review of influencing factors. *Eu J of Pros and Rest Dent* 2018;26:101-21.
7. D'haese, J. Accuracy and complications using computer- designed stereolithographic surgical guides for oral rehabilitation by means of dental implants: a review of the literature. *Clin Implant Dent Relat Res* 2012;14:321–35.
8. Jang Y, et al. “Evaluation of the Marginal and Internal Fit of a Single Crown Fabricated Based on a Three-Dimensional Printed Model.” *J of Adv Prostho* 108;10:5:367-73.
9. Griffith, R. “SLA vs. DLP: Which One Is Better?” *3D Insider*, 4 Sept. 2019, 3dinsider.com/sla-vs-dlp/.
10. Duret F, et al. CAD/CAM Imaging in Dentistry. *Curr Opin Dent*. 1991;1;150-54.
11. Miyazaki, T. et al. A review of dental CAD/CAM: Current status and future perspectives from 20 years of experience. *Dent Mater J* 2009;28:44–56.

12. Azari A, et al. The evolution of rapid prototyping in dentistry: A review. *Rapid Prototyp J* 2009;15:216-25.
13. Renne W, et al. "Evaluation of the Accuracy of 7 Digital Scanners: An in Vitro Analysis Based on 3- Dimensional Comparisons." *J of Prosthet Dent*, 2017;118;1:36-42.
14. International Organization for Standardization. ISO 5725-1. Accuracy (trueness and precision) of measurement methods and results - Part 1: General principles and definitions. Geneva: International Organization for Standardization; 1994.
15. Ender A, et al. Accuracy of complete-arch dental impressions: a new method of measuring trueness and precision. *J Prosthet Dent* 2013;109:121-8.
16. "Understanding Accuracy, Precision, and Tolerance in 3D Printing." Formlabs, formlabs.com/blog/understanding-accuracy-precision-tolerance-in-3d-printing/.
17. Goodacre B, et al. "Comparison of Denture Tooth Movement between CAD-CAM and Conventional Fabrication Techniques." *J of Prosthet Dent* 2018;1;108-15.
18. Al-Imam H, et al. "Accuracy of Stereolithography Additive Casts Used in a Digital Workflow." *J of Prosthet Dent* 2018;119;4:580-585.
19. Park M. "Three-Dimensional Comparative Study on the Accuracy and Reproducibility of Dental Casts Fabricated by 3D Printers." *J of Prosthet Dentistry* 2018;119;5: 861.e1–861.e7.
20. Norvell N, et al. "Comparison of Digital Surface Displacements of Maxillary Dentures Based on Noninvasive Anatomic Landmarks." *J of Prosthet Dent* 2018;120;1:123-31.
21. Jin S, et al. "Accuracy (Trueness and Precision) of Dental Models Fabricated Using Additive Manufacturing Methods." *Int J of Comp Dent* 2018;21;2:107-113.
22. "Support Documentation - Learn about 3Shape Product Specs." 3Shape, www.3shape.com/en/support-docs.

23. Form Wash Time Settings. 2020, support.formlabs.com/s/article/Form-Wash-Time-Settings?language=en_US.
24. Form Cure Time And Temperature. 2020, support.formlabs.com/s/article/Form-Cure-Time-and-Temperature-Settings?language=en_US.
25. Malik, J. Comparison of Accuracy Between a Conventional and Two Digital Intraoral Impression Techniques. *Int J Prosthodont* 2018;31;2:107-113.
26. Sommacal, B. Evaluation of Two 3D Printers for Guided Implant Surgery. *Int J Oral Maxillofac Implants* 2018;33:743-746.
27. Schwartz H, et al. "Linear Dimensional Accuracy of Epoxy Resin and Stone Dies." *J of Prosthet Dent* 1981;45;6:621-25.
28. Caruso, J. "3DRPD." 3DRPD, 2020, www.3drpd.com/.
29. SprintRay Inc., 23 July 2018, sprintray.com/blog/page/7/.
30. "Geomagic Control X." 3D Systems, www.3dsystems.com/software/geomagic-control-x